ELSEVIER

Journal of Alloys and Compounds 344 (2002) 186–189

Journal of ALLOYS AND COMPOUNDS

www.elsevier.com/locate/jallcom

Synthesis and characterization of nanosized powders of yttria-doped zirconia

S.K. Tadokoro*, E.N.S. Muccillo

Energy and Nuclear Research Institute-CCTM, Multidisciplinary Center for the Development of Ceramic Materials, C.P. 11049, Pinheiros,
São Paulo, SP 05422-970, Brazil

Abstract

Zirconia–3 mol% yttria nanosized powders have been prepared following a chemical route. The aim of this work is to optimize the techniques of solid solution synthesis and processing to obtain nanophase sintered ceramics without using milling or other special procedures. To ascertain this, several characterization techniques have been used. The electrical resistivity of polycrystalline specimens was compared to that of a single crystal of similar chemical composition. The main results show that a monomodal distribution of pore sizes has been obtained. Total stabilization of the tetragonal phase and nanophase sintered ceramics with relative densities of 98% were prepared by sintering at temperatures lower than 1200 °C. The main conclusion is that the optimization of the synthesis and processing techniques play a key role for improvement of chemical and physical properties of solid electrolytes prepared by chemical techniques.

Keywords: Nanostructures; Precipitation; Scanning electron microscopy; Ionic conduction

1. Introduction

Zirconia–yttria ceramics have been proposed for a number of applications due to the combination of mechanical, thermal, electrical and optical properties. Several efforts have been made over the last years for the optimization of synthesis and processing procedures to improve chemical and microstructural homogeneities. As a result, the preparation of ultrafine powders has lead to unusual properties like superplasticity and others [1]. Several techniques have been proposed for the synthesis of ultrafine powders allowing for obtaining nanophase ceramics. Nanophase zirconia doped with 3 mol% yttria (Y-TZP) sintered ceramics have been prepared by the pyrolysis of alcoholic solutions [2], sol–gel [3], combustion [4], and inert gas condensation [5] techniques. However, the coprecipitation of salts is the most used technique for preparing zirconia-based solid solutions for industrial scale. Some works in the literature suggest the use of this technique for the synthesis of nanophase Y-TZP ceramics. In these works, however, the formation of hard agglomerates during the synthesis process induces one of the additional step procedures: ultrasonic dispersion [6], attritor milling [6–8] and hydrothermal recrystallization [7,9].

In this work, zirconia–3 mol% yttria solid solutions have been prepared by the coprecipitation technique. The main purpose is to obtain highly sinterable nanosized powders with controlled agglomeration in order to produce nanophase ceramics without using special procedures during processing.

2. Experimental

$ZrOCl_2 \cdot 8H_2O$ (>99%) and Y_2O_3 (>99.9%) were used as starting materials. Yttrium nitrate solution was prepared by dissolution of the starting material in nitric acid. All other reagents were of analytical grade. For the synthesis of the solid solutions containing 3 mol% yttria, the coprecipitation technique in water medium followed by azeotropic distillation were used. After precipitation completion, the gel remained under vigorous stirring for 2 h. The precipitate was washed with a 10 vol%. ammonium hydroxide solution until complete elimination of Cl^- ions. Dehydration was carried out with alcoholic solutions for the interchange of hydroxyl and alkoxy groups. Then, the gel was dispersed in *n*-butyl alcohol and distilled. The precipitate was dried at 45 °C and gently deagglomerated

---

*Corresponding author.

0925-8388/02/$ – see front matter
PII: S0925-8388(02)00337-7

in an agate mortar. During the experiments, 26 variables were controlled to ensure reproducibility. These variables have been selected from previous works [10–13]. However, most of the combinations of these variables found in the literature do result in powders containing a significant amount of hard agglomerates. These hard agglomerates are responsible for the poor densification of ceramic compacts. This is the reason for the additional step (ultrasonic dispersion, milling or hydrothermal treatment) used in most works where solid solutions are prepared by the coprecipitation technique. After many combinations of the variables involved in the precipitation process, we have found best results for: low-concentrations of the cation (0.1 g l^{-1}) and precipitant (1 g l^{-1}) solutions; precipitation pH greater than 9; a suitable washing cycle with ammonium solution–absolute ethanol–isopropyl alcohol of 4:2:2. The azeotropic distillation was quite important to remove residual water from the gel. The size of the prepared batch is also important as many of these variables are best controlled employing low-size batches.

Cylindrical specimens were prepared by uniaxial and isostatic pressing. The sintering was carried out in air for 5 h at selected temperatures.

The specific surface area of calcined powders was obtained by the BET (Brunauer, Emmett, Teller) method (ASAP 2010, Micromeritics). The BJH (Barret, Joyner, Halenda) method was used for obtaining the pore size distribution. The linear shrinkage (DIL 402 E/7, Netzsch) of powder compacts was followed up to 1500 °C with heating and cooling rates of 8 °C and 15 °C min^{-1}, respectively.

Fractured or polished and thermally etched surfaces of sintered specimens were observed in a scanning electron microscope (LEO 440I, Oxford). The grain size distribution was calculated over ~1000 grains by a home made program based on the Saltikov statistical analysis. Raman spectroscopy (Renishaw Raman Microscope System 3000 coupled to an Olympus BH-2 microscope and to a CCD detector cooled by Peltier) was used to characterize the phase composition in sintered specimens. An Ar^+ laser (Omnichrome, model 170) with an exciting radiation of 514.5 nm was used.

Electrical resistivity measurements were carried out in a HP4192A impedance analyzer between 5 Hz and 13 MHz in the 280–540 °C temperature range. The results were analyzed in the impedance mode, using a special software [14]. Silver paste was used as electrode material.

3. Results and discussion

The value of specific surface area determined by the BET method is 132.5 m^2 g^{-1} after calcining at 500 °C for 1 h. This calcination profile was selected from thermal analysis results.

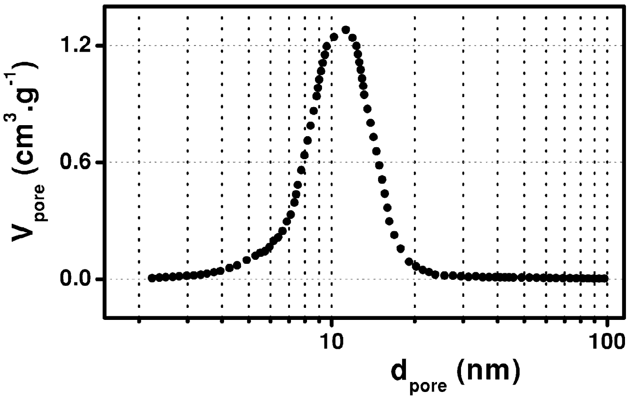

Fig. 1. Pore size distribution curve obtained by the BJH method after calcining the powder.

The pore size distribution determined by the BJH method assuming a cylindrical pore model is shown in Fig. 1. A monomodal distribution of pore sizes can be seen in this curve. In general, zirconia-based solid solutions present a bimodal distribution of pore sizes assigned to intra- and interagglomerate pores. The latter are hardly removed and usually cause an increase in time and/or temperature required for complete densification of these ceramics. The present result is attributed to the use of optimized parameters during synthesis and to the complete elimination of residual water from the precipitate by azeotropic distillation.

The linear shrinkage of a powder compact and its derivative are shown in Fig. 2. Total shrinkage is 27% and occurs in a temperature interval of 550–1255 °C. The maximum shrinkage rate occurs at 1075 °C.

Fig. 3 is a representative micrograph of the fracture surface of a sintered specimen (sintering temperature, 1170 °C). The main characteristic features are low-porosity and grains with uniform shape and similar average size.

Sintering of the compacted powders at temperatures between 1170 and 1200 °C resulted in high densification. The specimen sintered at 1200 °C for 5 h, for example,

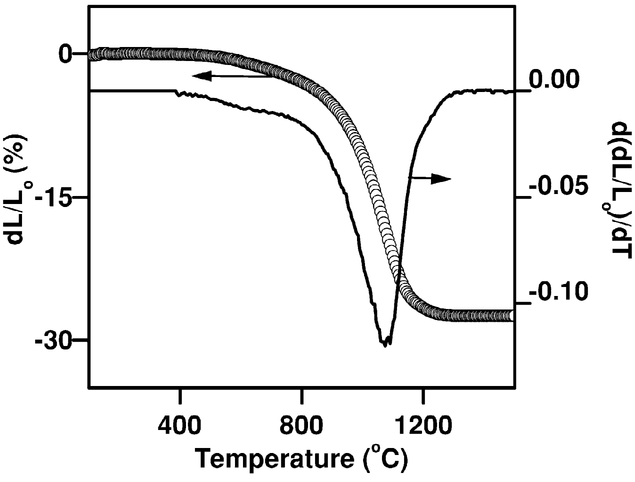

Fig. 2. Curves of linear shrinkage and its derivative for powder compacts.

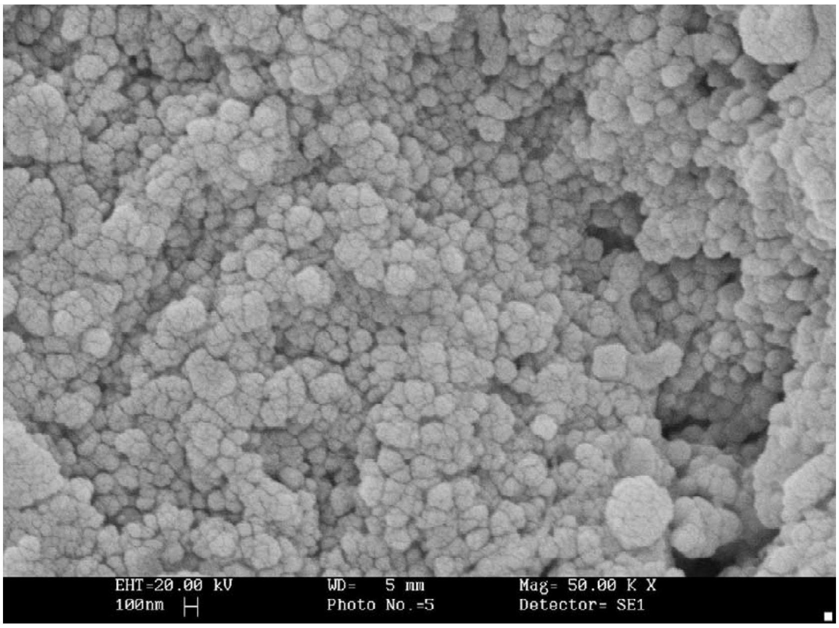

Fig. 3. Scanning electron micrograph of a fracture surface of Y-TZP sintered specimen. Sintering temperature, 1170 °C.

reached 99.5% relative density (assuming a theoretical density value of 6.12 g cm^{-3}), and an average grain size of 130±50 nm.

Fig. 4 shows the Raman spectrum of a sintered specimen. Six bands of the zirconia–yttria solid solution can be seen, including that centered at 460 nm, which is characteristic of the tetragonal phase. This result shows that total stabilization of the tetragonal phase has been achieved for this composition and sintering condition.

Typical impedance diagrams for polycrystalline and single crystal specimens are shown in Fig. 5. Numbers positioned over experimental points are the decimal logarithm of the frequency, in Hz. The high-frequency semicircle is due to lattice or intragranular resistivity either for the single crystal or sintered specimens. The low-frequency semicircle is assigned to the intergranular resistivity due to the blocking of charge carriers at grain boundaries. The comparatively large diameter of this low-frequency semicircle is a consequence of the small average grain size of this specimen. As shown in the insert (Fig. 5), there is an overlap of both semicircles, and a careful resolution of these diagrams is quite important for obtaining a precise value for the activation energy of the intragranular resistivity.

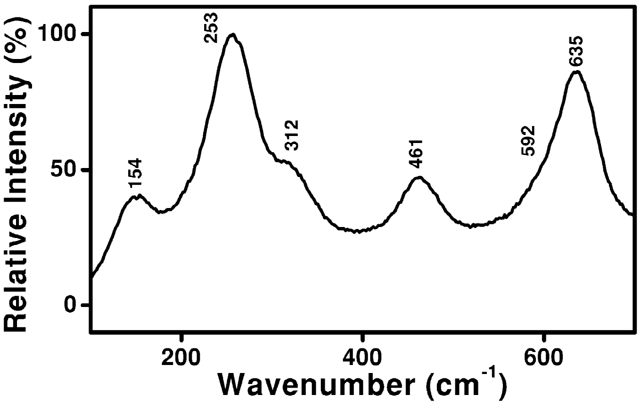

Fig. 4. Raman spectrum of a specimen sintered at 1170 °C.

The activation energy values for intra- and intergranular resistivity were calculated from the Arrhenius plots of the electrical resistivity resulting in 0.86 and 1.07 eV, respectively. These figures are in general agreement with values obtained for a sintered specimen prepared by inert gas condensation technique [15]. The activation energy for the lattice resistivity of the single crystal is 0.91 eV. Although single- and polycrystalline specimens have the same chemical composition, the exact phase composition of the single crystal cannot be ascertained because the cooling rate of the process for growing this crystal is not known. This is a possible reason for the difference observed in the activation energy values for conduction in both materials.

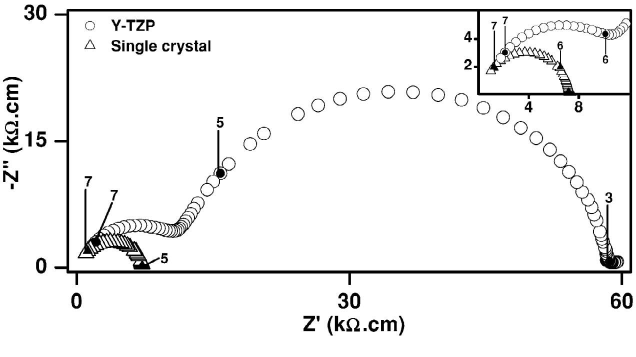

Fig. 5. Impedance spectroscopy diagrams for single crystal and polycrystalline specimen sintered at 1170 °C.

4. Conclusions

A careful selection of the synthesis and processing parameters is a key role for preparing Y-TZP nanosized powders with suitable chemical and microstructural properties. Specimens having high surface area and monomodal distribution of pore sizes have been obtained without using any milling or other special procedures. Reactive ceramic powders with these characteristics allow for manufacturing ceramics with high sinterability, reduced average grain size, and high chemical and microstructural homogeneities.

Acknowledgements

To FAPESP (92/02962-6, 94/05929-5, 95/05635-4, 99/10798-0) that sponsored most of the facilities used in this work. S.K.T. acknowledges FAPESP (98/09976-9) for the scholarship. To Ceres Co. for the single crystal. To CNEN and CNPq (300934/94-7).

References

[1] R.D. Shull, Nanostruct. Mater. 2 (1993) 213.
[2] W. Li, L. Gao, J.K. Guo, Nanostruct. Mater. 10 (1998) 1043.
[3] S.D. Ramamurthi, Z. Xu, D.A. Payne, J. Am. Ceram. Soc. 73 (1990) 2760.
[4] S. Jiang, W.A. Shulze, V.R.W. Amarakoon, G.C. Stangle, J. Mater. Res. 12 (1997) 2374.
[5] H. Hahn, Nanostruct. Mater. 9 (1997) 3.
[6] M.J. Mayo, Mater. Design 14 (1993) 323.
[7] C.D.S. Ransijn, A.J.A. Winnubst, B. Kerkwij, A.J. Burggraaf, H. Verwey, J. Eur. Ceram. Soc. 17 (1997) 831.
[8] P. Durán, M. Villegas, J.F. Fernández, F. Capel, C. Moure, Mater. Sci. Eng. A232 (1997) 168.
[9] N.M.R. Boutz, R.J.M.O. Scholtenhuis, A.J.A. Winnubst, A.J. Burggraaf, Mater. Res. Bull. 29 (1994) 31.
[10] T. Suzuki, S. Osaka, N. Aikawa, Applied European Patent 0171736A2, 1986.
[11] D.M. Ávila, E.N.S. Muccillo, Thermochim. Acta 256 (1995) 391.
[12] E.N.S. Muccillo, D.M. Ávila, Cer. Int. 25 (1999) 345.
[13] E.N.S. Muccillo, R. Muccillo, D.M. Ávila, Mater. Sci. Forum 299/300 (1999) 70.
[14] M. Kleitz, J.H. Kennedy, in: P. Vashishta, J.N. Mundy, G.K. Shenoy (Eds.), Fast Ion Transport in Solids, Electrodes and Electrolytes, North-Holland, Amsterdam, 1979, p. 185.
[15] P. Mondal, A. Klein, W. Jaegermann, H. Hahn, Solid State Ionics 118 (1999) 331.